Role of Configurational Gating in Intracomplex Electron Transfer from Cytochrome *c* to the Radical Cation in Cytochrome *c* Peroxidase†

Hongkang Mei,‡ Kefei Wang,‡ Nicole Peffer,‡ Gresham Weatherly,§ David S. Cohen,§ Mark Miller,|| Gary Pielak,§ Bill Durham,‡ and Francis Millett*,‡

Department of Chemistry and Biochemistry, University of Arkansas, Fayetteville, Arkansas 72701, Department of Chemistry, University of North Carolina, Chapel Hill, North Carolina 27599-3290, and Monsanto/NutraSweet Kelco Company, 8355 Aero Drive, San Diego, California 92123-1718

Received December 21, 1998; Revised Manuscript Received March 30, 1999

ABSTRACT: Electron transfer within complexes of cytochrome *c* (Cc) and cytochrome *c* peroxidase (CcP) was studied to determine whether the reactions are gated by fluctuations in configuration. Electron transfer in the physiological complex of yeast Cc (yCc) and CcP was studied using the Ru-39-Cc derivative, in which the H39C/C102T variant of yeast iso-1-cytochrome *c* is labeled at the single cysteine residue on the back surface with trisbipyridylruthenium(II). Laser excitation of the 1:1 Ru-39-Cc−CcP compound I complex at low ionic strength results in rapid electron transfer from Ru^{II*} to heme *c* Fe^{III}, followed by electron transfer from heme *c* Fe^{II} to the Trp-191 indolyl radical cation with a rate constant k_{eta} of 2×10^6 s^{-1} at 20 °C. k_{eta} is not changed by increasing the viscosity up to 40 cP with glycerol and is independent of temperature. These results suggest that this reaction is not gated by fluctuations in the configuration of the complex, but may represent the elementary electron transfer step. The value of k_{eta} is consistent with the efficient pathway for electron transfer in the crystalline yCc−CcP complex, which has a distance of 16 Å between the edge of heme *c* and the Trp-191 indole [Pelletier, H., and Kraut, J. (1992) *Science 258*, 1748−1755]. Electron transfer in the complex of horse Cc (hCc) and CcP was examined using Ru-27-Cc, in which hCc is labeled with trisbipyridylruthenium(II) at Lys-27. Laser excitation of the Ru-27-Cc−CcP complex results in electron transfer from Ru^{II*} to heme *c* Fe^{II} with a rate constant k_1 of 2.3×10^7 s^{-1}, followed by oxidation of the Trp-191 indole to a radical cation by Ru^{III} with a rate constant k_3 of 7×10^6 s^{-1}. The cycle is completed by electron transfer from heme *c* Fe^{II} to the Trp-191 radical cation with a rate constant k_4 of 6.1×10^4 s^{-1}. The rate constant k_4 decreases to 3.4×10^3 s^{-1} as the viscosity is increased to 84 cP, but the rate constants k_1 and k_3 remain the same. The results are consistent with a gating mechanism in which the Ru-27-Cc−CcP complex undergoes fluctuations between a major state A with the configuration of the hCc−CcP crystalline complex and a minor state B with the configuration of the yCc−CcP complex. The hCc−CcP complex, state A, has an inefficient pathway for electron transfer from heme *c* to the Trp-191 indolyl radical cation with a distance of 20.5 Å and a predicted value of 5×10^2 s^{-1} for k_{4A}. The observed rate constant k_4 is thus gated by the rate constant k_a for conversion of state A to state B, where the rate of electron transfer k_{4B} is expected to be 2×10^6 s^{-1}. The temperature dependence of k_4 provides activation parameters that are consistent with the proposed gating mechanism. These studies provide evidence that configurational gating does not control electron transfer in the physiological yCc−CcP complex, but is required in the nonphysiological hCc−CcP complex.

The electron transfer reaction between two redox proteins involves at least three steps: (1) formation of a reactant complex of the two proteins, (2) electron transfer within the reactant complex in forming the product complex, and (3) dissociation of the product complex. It has often been assumed that the second step, intracomplex electron transfer, takes place within a static reactant complex, in which case the observed rate constant is caused by the actual electron transfer event. However, a number of cases have been observed in which the reactant complex is not static, but is undergoing dynamic fluctuations in configuration (defined as protein−protein orientation in the bound complex) or conformation (defined as the tertiary structure of each protein). If the reaction is rate-limited by the dynamic fluctuations rather than by the actual electron transfer event, then it is said to be gated (*1*, *2*). Kostić and co-workers found that the rate constants for intracomplex electron transfer between zinc−cytochrome *c* (Zn-Cc) and either plastocyanin or cytochrome b_5 decrease significantly with increasing viscosity, indicating gating by dynamic fluctuations in configuration (*3*−*5*). Harris et al. (*6*) also reported evidence supporting configurational gating in the complex of ruthenium-labeled cytochrome *c* and plastocyanin. Davidson and co-workers reported that electron transfer between methylamine dehydrogenase and amicyanin is not gated, but may be coupled to rapid reorientation of the tryptophan trpytophylquinone prosthetic groups (*2*, *7*, *8*). This study was

† This work was supported by NIH Grants GM20488 (F.M. and B.D.) and GM42501 (G.P.) and NSF Grant MCB 91192 (M.M.).

‡ University of Arkansas.

§ University of North Carolina.

|| Monsanto/NutraSweet Kelco Co.

10.1021/bi983002t CCC: $18.00
Published on Web 05/04/1999

Scheme 1

$$(Fe^{IV}{=}O,R^{\bullet+}) + c^{II} \underset{k_d}{\overset{k_f}{\rightleftarrows}} (Fe^{IV}{=}O,R^{\bullet+}){:}c^{II} \xrightarrow{k_{eta}} (Fe^{IV}{=}O,R){:}c^{III} \underset{k_f}{\overset{k_d}{\rightleftarrows}} (Fe^{IV}{=}O,R) + c^{III}$$

$$(Fe^{IV}{=}O,R) + 2\,H^{+} \overset{K}{\rightleftarrows} (Fe^{III},R^{\bullet+}) + H_2O$$

$$(Fe^{III},R^{\bullet+}) + c^{II} \underset{k_d}{\overset{k_f}{\rightleftarrows}} (Fe^{III},R^{\bullet+}){:}c^{II} \xrightarrow{k_{eta}} (Fe^{III},R){:}c^{III} \underset{k_f}{\overset{k_d}{\rightleftarrows}} (Fe^{III},R) + c^{III}$$

undertaken to determine whether gating occurs during electron transfer within the physiological complex of yeast iso-1-cytochrome *c* (yCc)[1] and cytochrome *c* peroxidase (CcP), and the nonphysiological complex of horse Cc and CcP.

The reaction between yCc and CcP is an important prototype for the study of interprotein electron transfer because of the extensive spectroscopic and structural characterization of the individual proteins as well as their 1:1 complex (*9*, *10*). In the first step of the reaction, the resting ferric state of CcP is oxidized by hydrogen peroxide to CMPI(Fe^{IV}=O,$R^{\bullet+}$), which contains an oxyferryl heme, Fe^{IV}=O, and a radical cation, $R^{\bullet+}$, located on the indole group of Trp-191 (*11*−*17*). The radical cation and oxyferryl heme in CMPI are then sequentially reduced by two molecules of ferrocytochrome *c* (Cc^{II}). The reduction of CMPI has been studied using Ru-Cc derivatives labeled with a ruthenium trisbipyridyl complex (*18*, *19*). Photoexcitation of the Ru-Cc derivative leads to formation of the metal-to-ligand charge transfer state, Ru^{II*}, which is a strong reducing agent and rapidly transfers an electron to the Cc ferric heme group (*20*). All of the Ru-Cc derivatives were found to initially reduce the Trp-191 radical cation in CMPI(Fe^{IV}=O,$R^{\bullet+}$) as shown in Scheme 1 (*18*, *19*). CMPII(Fe^{IV}=O,R) is then converted to CMPII(Fe^{III},$R^{\bullet+}$) by intramolecular electron transfer, followed by reduction of the radical cation in CMPII(Fe^{III},$R^{\bullet+}$) by a second molecule of Cc^{II} which gives the resting enzyme (*21*). Stopped-flow studies have demonstrated that native hCc and yCc initially reduce the radical cation in CMPI according to Scheme 1 under all conditions of ionic strength and pH (*22*, *24*, *25*). The results of earlier studies (*26*−*28*) have also been shown to be consistent with initial reduction of the radical cation in CMPI (*22*). The rate constant for electron transfer to the Trp-191 radical cation in the physiological yCc−CcP complex (k_{eta}) was found to be 2×10^6 s^{-1} using yeast Ru-39-Cc, which is labeled on the back surface where it does not interfere in the interaction with CcP (*22*). The reaction between native yCc and CcP measured over a wide range of conditions using stopped-flow spectroscopy and steady-state kinetics is in quantitative agreement with Scheme 1, using the rate constants k_{eta}, K, k_f, and k_d measured with Ru-39-Cc (*22*, *23*, *29*).

[1] Abbreviations: Cc, cytochrome *c*; hCc, horse Cc; yCc, yeast iso-1-cytochrome *c*; CcP, cytochrome *c* peroxidase; CcP(MI), recombinant CcP; CMPI, CcP compound I; CMPII, CcP compound II; Ru-39-Cc, Ru(bipyridine)$_2$[4,4′-dimethylbipyridine-Cys-39-(H39C/C102T)-yCc]; Ru-27-Cc, Ru(bipyridine)$_2$(4,4′-dicarboxybipyridine-Lys-27-hCc).

The X-ray crystal structure of the 1:1 complex of yCc and CcP revealed that the exposed heme edge of yCc is in van der Waals contact with CcP residues Ala-193 and Ala-194 at the center of the binding domain (*9*). Pelletier and Kraut proposed an electron transfer pathway extending from the yCc heme methyl group through CcP residues Ala-194, Ala-193, and Gly-192 to the indole group on Trp-191, which is in van der Waals contact with the heme group (*9*). Mutagenesis studies demonstrated that the yCc binding site identified in the crystal structure is used for reduction of both the Trp-191 radical cation and the oxyferryl heme in solution (*22*, *30*). Thus, both steps in the complete reduction of CMPI involve electron transfer from yCc^{II} to the Trp-191 radical cation according to Scheme 1 using the binding site and electron transfer pathway identified in the crystal structure.

In this study, electron transfer within a 1:1 complex of horse Ru-27-Cc and CcP was measured by using a novel method involving photoreduction of heme *c* Fe^{III} by Ru^{II*}, oxidation of Trp-191 to the radical cation by Ru^{III}, followed by electron transfer from heme *c* Fe^{II} to the Trp-191 radical cation (*31*). The rate constant for electron transfer from heme *c* Fe(II) to the Trp-191 radical cation decreases significantly with increasing viscosity, while the rate constant for electron transfer between Trp-191 and Ru(III) is independent of viscosity. A gating mechanism is proposed in which the dominant configuration of the complex is that of the hCc−CcP crystal structure which has a 3 Å gap between the edge of heme *c* and Ala-193, and would have a very small rate for electron transfer. Fluctuations to a configuration more like that of the yCc−CcP complex would allow rapid electron transfer. In contrast, intracomplex electron transfer from yeast Ru-39-Cc to the Trp-191 radical cation is independent of viscosity, suggesting that electron transfer in the physiological yCc−CcP complex is not limited by configurational gating.

EXPERIMENTAL PROCEDURES

Materials. Yeast iso-1-Ru-39-Cc was prepared as described by Geren et al. (*32*). Horse Ru-27-Cc was prepared by the method of Pan et al. (*33*). The parent enzyme and mutants D34N, D290N, E291Q, and A193F were prepared as described previously (*30*, *34*).

Laser Flash Photolysis Studies. Flash photolysis studies were carried out as described by Durham et al. (*20*), Wang et al. (*22*), and Liu et al. (*31*). The excitation flash was provided either by the second harmonic of a Nd:Yag laser with a width of 10 ns and a wavelength of 532 nm or by a

Scheme 2

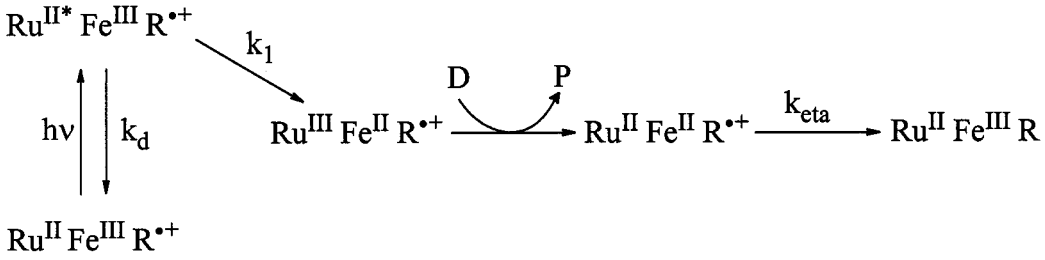

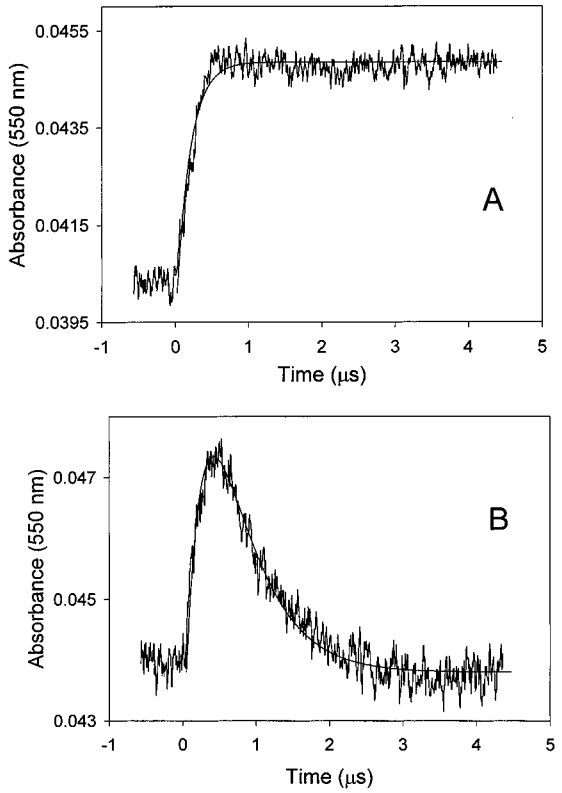

FIGURE 1: Photoinduced electron transfer from Ru-39-Cc^{II} to CMPI in glycerol. (A) A solution containing 11 μM Ru-39-Cc and 12.5 μM CcP in 2 mM sodium phosphate (pH 7.0), 5 mM aniline, and 76% glycerol at 20 °C was excited with a 480 nm laser flash. The smooth curve is the best fit to Scheme 2 with a $k_1 + k_d$ of 6.5 × 10^6 s^{-1}, and k_{eta} set to zero. (B) CcP (12.5 μM) was treated with 12.5 μM H_2O_2 to form CMPI and then added to a solution containing 11 μM Ru-39-Cc in 2 mM sodium phosphate (pH 7.0), 5 mM aniline, and 76% glycerol at 20 °C. The 550 nm transient was recorded within 10 s of mixing. CMPI was stable for 1 min under these conditions. The smooth line is the best fit to Scheme 2 with a $k_1 + k_d$ of 6.5 × 10^6 s^{-1} and a k_{eta} of 1.5 × 10^6 s^{-1}.

phase R model DL1400 flash lamp-pumped dye laser producing a 480 nm light flash with a width of 500 ns. The probe source was a pulsed 75 W xenon arc lamp, and the photomultiplier detector had a response time of 20 ns. A 100 W quartz halogen lamp was used as the probe source for slower reactions in the 1 μs to 1 s time domain. The sample was placed in a glass semi-microcuvette with a path length of 1 cm. The experimental transients were corrected for the finite response time of the laser and detection system using convolution methods and fitted by the appropriate theoretical equations as described previously (*20*, *22*, *31*).

RESULTS

Photoinduced Electron Transfer in the Yeast Ru-39-Cc−CcP Complex. The intracomplex electron transfer reaction between yeast Ru-39-Cc and the Trp-191 radical cation in CcP CMPI was assessed using previously described methods (*22*). Photoexcitation of a solution containing 10 μM Ru-39-Cc and 12 μM resting-state CcP in 1 mM sodium phosphate (pH 7.0), 5 mM aniline, and 76 wt % glycerol resulted in a rapid increase in the absorbance at 550 nm with a rate constant $k_1 + k_d$ of (6.5 ± 1.0) × 10^6 s^{-1} (Figure 1A). This is consistent with Scheme 2, in which the sacrificial reducing agent aniline reduces Ru(III) and prevents the back reaction with Fe^{II}. When the same experiment was performed on a complex of Ru-39-Cc and CcP CMPI in 76% glycerol, the rapid increase in absorbance at 550 nm was followed by an exponential decrease, indicating electron transfer from heme *c* Fe(II) to the Trp-191 radical cation in CMPI according to Scheme 2 (Figure 1B). The 550 nm transient was fit to Scheme 2 with a $k_1 + k_d$ of (6.5 ± 1.0) × 10^6 s^{-1} and a k_{eta} of (1.5 ± 0.5) × 10^6 s^{-1} (*22*). The transient was recorded within 10 s of formation of CMPI by addition of 1 equiv of H_2O_2 to resting-state CcP. Control experiments in which a diode array spectrophotometer was used indicated that CMPI was stable for at least 1 min under these conditions. The same results were obtained using lower concentrations of glycerol, and in the absence of glycerol, where k_{eta} equals (2.0 ± 0.5) × 10^6 s^{-1} (Table 1). Thus, the rate constant, k_{eta}, for intracomplex electron transfer from Ru-39-Cc to the Trp-191 radical cation in CMPI is independent of viscosity. The same value of k_{eta} was also obtained at 1 °C in the absence of glycerol (Table 1).

Table 1: Photoinduced Electron Transfer from Ru-39-Cc to CMPI in the Presence of Glycerol[a]

temperature (°C)	glycerol (wt %)	viscosity (cP)	k_{eta} (×10^6 s^{-1})
20	0	1.0	2.0 ± 0.5
20	68	18.4	2.0 ± 0.5
20	76	40.5	1.5 ± 0.5
1.0	0	1.73	2.0 ± 0.5

[a] k_{eta} was measured as described in the legend of Figure 1 in 2 mM sodium phosphate (pH 7) and 0−76% glycerol. The viscosities of glycerol solutions at 20 and 1 °C are given in refs *43* and *44*, respectively.

Photoinduced Electron Transfer in Horse Ru-27-Cc−CcP Complexes. Flash photolysis of Ru-27-Cc results in electron transfer from Ru(II*) to Fe(III), followed by the back reaction from Fe(II) to Ru(III) according to Scheme 3 (without CcP) with rate constants k_1 of 2.3 × 10^7 s^{-1}, k_2 of 2.2 × 10^7 s^{-1}, and k_d of 2.1 × 10^7 s^{-1} (Figure 2A) (*31*). The 550 nm transient obtained with the 1:1 Ru-27-Cc−CcP complex at low ionic strengths indicated that the rapid reoxidation of heme *c* was decreased to about 50% of the total (Figure 2B). This was followed by a much slower phase, resulting in complete reoxidation (Figure 2C). Electron transfer within this 1:1 Ru-27-Cc−CcP complex has been previously shown

Scheme 3

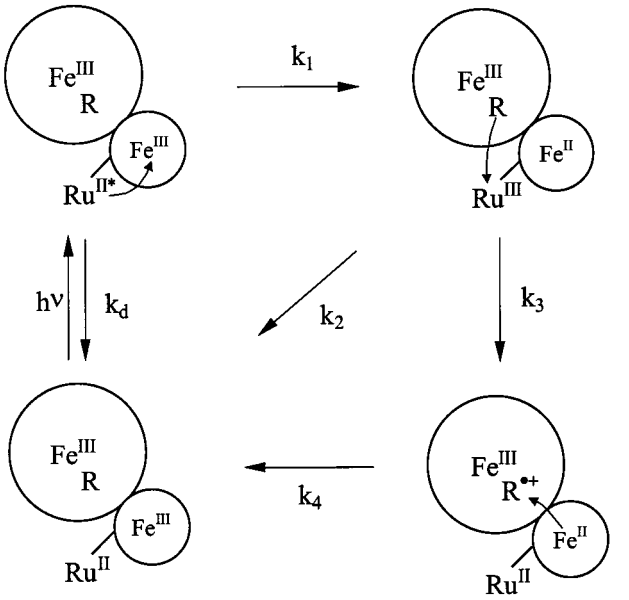

Table 2: Effect of Viscosity on Photoinduced Electron Transfer in the Ru-27-Cc−CcP Complex[a]

glycerol (wt %)	k_1 ($\times 10^7$ s^{-1})	k_2 ($\times 10^7$ s^{-1})	k_d ($\times 10^7$ s^{-1})	k_3 ($\times 10^6$ s^{-1})	k_4 ($\times 10^3$ s^{-1})
0	2.0 ± 0.5	2.4 ± 0.5	2.4 ± 0.5	7 ± 2	61 ± 6
80	2.1 ± 0.5	2.3 ± 0.6	2.5 ± 0.6	6 ± 2	4.3 ± 0.5

[a] The rate constants for photoinduced electron transfer in the Ru-27-CcP complex according to Scheme 4 were measured as described in the legend of Figure 2 in a solution containing 2 mM sodium phosphate (pH 7.0) and 0 or 80% glycerol with a viscosity of 60 cP at 20 °C (*33*).

to obey the mechanism given in Scheme 3 (*31*). Photoexcited Ru^{II*} rapidly transfers an electron to heme *c* Fe^{III} with rate constant k_1 to form Fe^{II} and Ru^{III}. The Ru^{III}, a strong oxidant, then accepts an electron from the indole group of Trp-191 with a rate constant k_3 to form the Trp-191 indolyl radical cation and Ru^{II}. The cycle is completed by electron transfer from heme *c* Fe^{II} to the radical cation with rate constant k_4. A unique set of values for the rate constants in Scheme 3 was obtained by simultaneously fitting the 434 nm transient for photoexcitation and recovery of Ru^{II}, the luminescence transient for the decay of Ru^{II*}, and the 550 nm transient for the reduction and reoxidation of heme *c* Fe^{III} using numerical integration methods described previously (*31*). The rate constants in 2 mM sodium phosphate at pH 7.0 and 20 °C are as follows: $k_1 = 2.3 \times 10^7$ s^{-1}, $k_2 = 2.2 \times 10^7$ s^{-1}, $k_d = 2.1 \times 10^7$ s^{-1}, $k_3 = 7.5 \times 10^6$ s^{-1}, and $k_4 = 6.1 \times 10^4$ s^{-1} (*31*).

Increasing the viscosity by addition of glycerol decreases the rate constant for electron transfer between heme *c* Fe(II) and the radical, k_4, from 6.1×10^4 s^{-1} at 1.0 cP to 3.4×10^3 s^{-1} at 84 cP (Figure 3). The other rate constants in Scheme 3, however, did not change with viscosity (Table 2). Most significantly, the intracomplex rate constant k_3 for electron transfer from the Trp-191 indole group in CcP to Ru(III) in Ru-27-Cc did not change up to the maximum viscosity. Increasing the viscosity with sucrose had a similar effect, decreasing k_4 to 6.6×10^3 s^{-1} at a viscosity of 40 cP, without affecting the other rate constants (Figure 3). At a

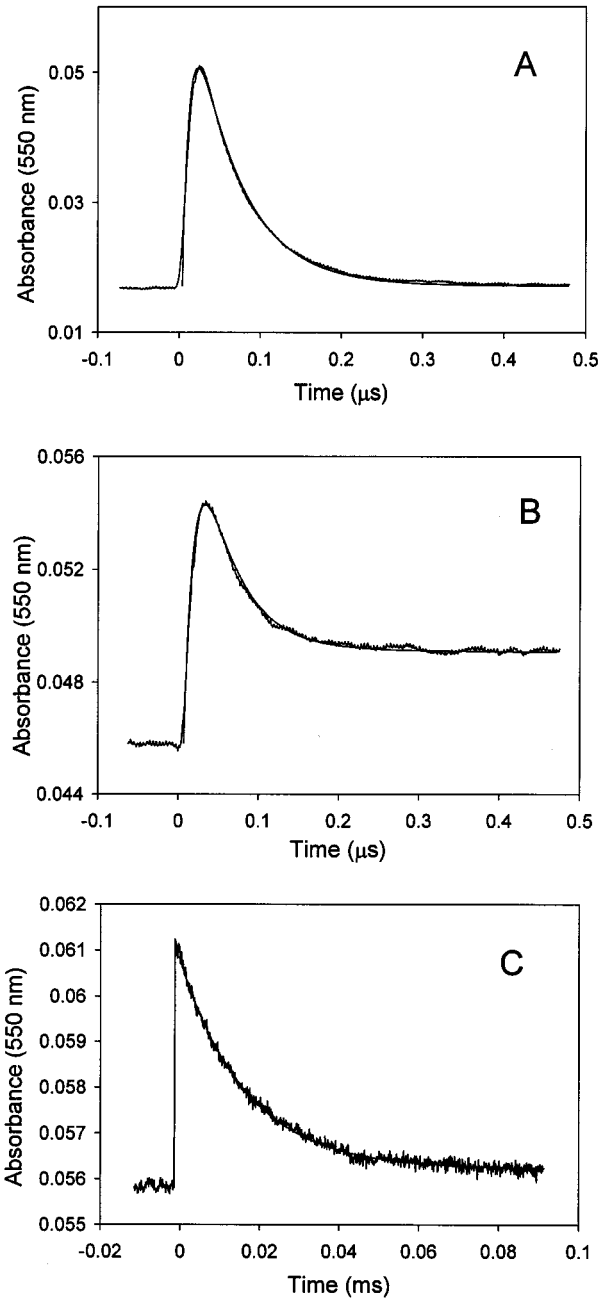

FIGURE 2: Photoinduced electron transfer in the Ru-27-Cc−CcP complex. (A) Ru-27-Cc (10 μM) in 2 mM sodium phosphate (pH 7.0) was excited with a 532 nm Nd:YAG laser flash with a 25 ns pulse width, and transients were recorded at 550, 556.5, and 434 nm. The smooth curve shows the best fit of the 550 nm transient to Scheme 3 with a k_1 of 2.3×10^7 s^{-1}, a k_2 of 2.2×10^7 s^{-1}, and a k_d of 2.1×10^7 s^{-1}. (B) Ru-27-Cc (10 μM) and 10 μM CcP were excited with a laser flash under the same conditions as described for panel A. (C) The same solution described for panel B was excited with a 480 nm flash from the dye laser, and the 550 nm transient was recorded on a longer time scale. The smooth lines in panels B and C are the best fit to Scheme 3 with a k_1 of 2.3×10^7 s^{-1}, a k_2 of 2.2×10^7 s^{-1}, a k_d of 2.1×10^7 s^{-1}, a k_3 of 7.5×10^6 s^{-1}, and a k_4 of 6.1×10^4 s^{-1}.

constant viscosity of 84 cP at an ionic strength of 2 mM, rate constant k_4 and the other rate constants were independent of protein concentration down to <1 μM. This result is an indication of electron transfer according to Scheme 3 within a 1:1 complex with a dissociation constant of <1 μM. The viscosity dependence of k_4 was fitted to the modified Kramer's equation (eq 1) (*4*):

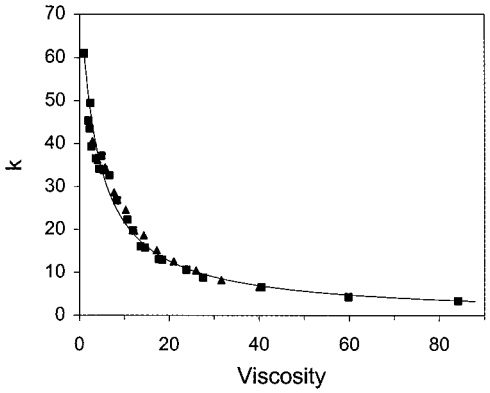

FIGURE 3: Effect of viscosity on photoinduced electron transfer in the Ru-27-Cc−CcP complex. The rate constant k_4 for Scheme 3 was measured as described in the legend of Figure 2 in the presence of glycerol (■) or sucrose (▲). The smooth curve is the best fit to eq 1 with a $\Delta G^{\ddagger}$ of 44.9 ± 0.2 kJ/mol, a σ of 4.0 ± 1.0 cP, and a k_{4A} of <1000 s^{-1}. The viscosities of glycerol and sucrose solutions are given in ref *43*.

Table 3: Effect of Glycerol on Photoinduced Electron Transfer in Complexes of Ru-27-Cc and CcP Mutants[a]

CcP mutant	k_4 ($\times 10^4$ s^{-1})	$\Delta G^{\ddagger}$ (kJ/mol)	σ (cP)
CcP(MI)	61 ± 6	44.9 ± 0.2	4.0 ± 1.0
D34N	134 ± 12	43.0 ± 0.2	0.6 ± 0.3
A193F	42 ± 4	45.8 ± 0.2	2.5 ± 0.8
E290N	40 ± 4	46.0 ± 0.2	4.0 ± 1.0
E291Q	67 ± 6	44.6 ± 0.2	2.4 ± 0.8

[a] The rate constant k_4 in the absence of glycerol and parameters in eq 1 were measured as described in the legend of Figure 3 at 20 °C.

$$k_4 = \frac{k_B T(1+\sigma)}{h(\eta+\sigma)} = \exp(-\Delta G^{\ddagger}/RT) + k_{4A} \qquad (1)$$

where k_B is Boltzmann's constant, h is Planck's constant, R is the gas constant, η is the viscosity in centipoise, σ is the protein friction in centipoise, and k_{4A} is the rate constant at infinite viscosity (*4*). The value of σ was found to be 4.0 ± 1.0 cP, and k_{4A} < 1000 s^{-1} (Figure 3 and Table 3).

The rate constant for electron transfer from heme *c* to the Trp-191 radical cation, k_4, was also affected by temperature, decreasing from 1.28 × 10^5 s^{-1} at 48 °C to 2.5 × 10^4 s^{-1} at 2 °C. The data were fitted to eq 2 using an Eyring plot (Figure 4).

$$k_4 = (k_B T/h)\exp(\Delta S^{\ddagger}/R)\exp(-\Delta H^{\ddagger}/RT) \qquad (2)$$

The activation parameters were found to have the following values: $\Delta H^{\ddagger}$ = 22.6 ± 1.4 kJ/mol, $\Delta S^{\ddagger}$ = −76 ± 5 J mol^{-1} K^{-1}, and $\Delta G^{\ddagger}$ = 44.9 ± 0.3 kJ/mol. The other rate constants in Scheme 3 were independent of temperature, within an error limit of ±20%. The viscosity dependence of k_4 was also measured at a constant temperature of 0 °C in solutions containing 0−84% glycerol (Figure 5). The value of the protein friction σ was 3.2 ± 1.0 cP, and k_{4A} < 1000 s^{-1} at 0 °C.

The viscosity dependence of k_4 suggests that gating controls electron transfer from heme *c* to the Trp-191 radical cation. To explore the nature of the gating, the viscosity dependence of a series of CcP mutants with changes in surface residues involved in the interaction with Ru-27-Cc was examined. The D34N and E290N mutations each cause

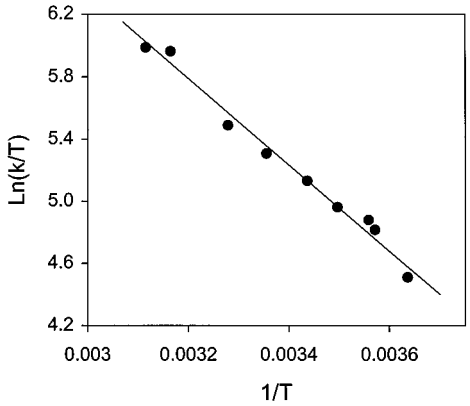

FIGURE 4: Effect of temperature on the photoinduced electron transfer in the Ru-27-Cc−CcP complex. The rate constant k_4 in Scheme 3 was measured as described in the legend of Figure 2 in 2 mM sodium phosphate (pH 7.0) in the absence of glycerol. The straight line is the best fit to eq 2 with a $\Delta H^{\ddagger}$ of 22.6 ± 1.4 kJ/mol and a $\Delta S^{\ddagger}$ of −76 ± 5 J mol^{-1} K^{-1}.

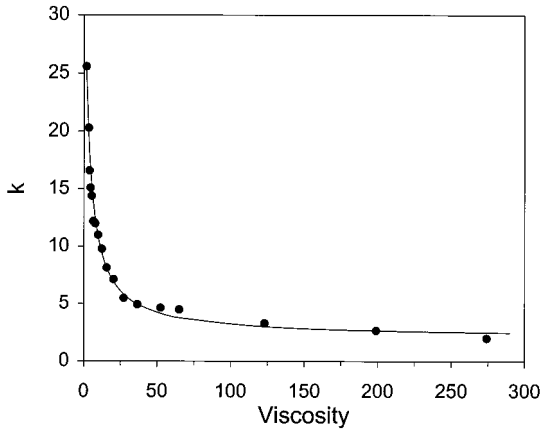

FIGURE 5: Effect of viscosity on the photoinduced electron transfer in the Ru-27-Cc−CcP complex at 0 °C. The rate constant k_4 for Scheme 3 was measured as described in the legend of Figure 3 in the presence of glycerol at 0 °C. The viscosity of glycerol solutions at 0 °C is given in ref *44*. The smooth curve is the best fit to eq 1 with a $\Delta G^{\ddagger}$ of 46.7 ± 0.2 kJ/mol, a σ of 3.2 ± 0.6 cP, and a k_{4A} of <1000 s^{-1}.

a significant increase in the dissociation constant of the complex with Ru-27-Cc, consistent with the involvement of Asp-34 and Glu-290 in the electrostatic interaction with Ru-27-Cc (*31*). Surprisingly, the D34N mutation increased k_4 to 1.4 × 10^5 s^{-1} at 22 °C in the absence of glycerol, compared with 6.1 × 10^4 s^{-1} for wild-type CcP, while the E290N mutation decreased k_4 to 4 × 10^4 s^{-1} (Table 3). The rate constant k_4 for all the mutants decreased with increasing viscosity, with the σ values shown in Table 3. The values of k_{4A} were less than 2000 s^{-1} for all the mutants.

DISCUSSION

Electron Transfer within the Yeast Ru-39-Cc−CcP Complex. The yeast Ru-39-Cc derivative was specifically designed to measure electron transfer within the physiological yeast Cc−CcP complex. Ru-39-Cc is labeled with trisbipyridine ruthenium at Cys-39 on the back surface of the protein where it does not interfere in the interaction with CcP. Both the dissociation constant for the high-affinity complex of Ru-39-Cc and CcP at low ionic strengths and the second-order rate constant for the reaction of Ru-39-Cc with the radical in CMPI at high ionic strengths are the same

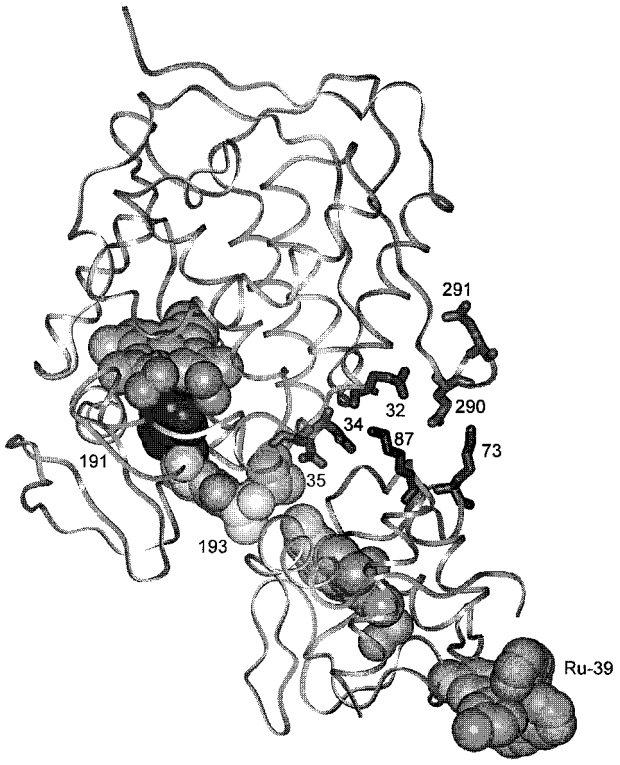

FIGURE 6: X-ray crystal structure of the yCc−CcP complex (*9*). The heme groups and CcP residues 191−194 are represented by CPK space-filling models, with the indole group of Trp-191 colored black, and the others in shades of gray. Selected CcP acidic residues and Cc lysines are represented by sticks. The ruthenium complex was attached to Cys-39 by molecular modeling.

as for wild-type yeast Cc (*22*). The rate constant for electron transfer from heme *c* to the Trp-191 indolyl radical cation within the 1:1 complex of Ru-39-Cc and CMPI (k_{eta}) is 2×10^6 s^{-1} in the absence of glycerol, and remains essentially unchanged as glycerol is added to increase the viscosity to 40 cP. Furthermore, k_{eta} is independent of temperature from 25 °C down to 0 °C, indicating that the energy of activation is close to zero. These observations suggest that k_{eta} is not controlled by configurational gating, but may represent the elementary electron transfer event. Previously examined systems in which electron transfer is limited by configurational gating are characterized by a large dependence of the rate constant on viscosity and temperature (*3*−*6*).

Site-directed mutagenesis studies have shown that the reaction between Ru-39-Cc and CcP CMPI in solution uses the binding domain identified in the crystal structure of the yeast Cc−CcP complex by Pelletier and Kraut (*9*, *22*). In this complex, the CBC methyl group on the exposed heme edge of yCc is in van der Waals contact with CcP residues Ala-193 and Ala-194 (Figure 6). Pelletier and Kraut proposed an electron transfer pathway that leads from the yCc heme methyl group through CcP residues Ala-194, Ala-193, and Gly-192 to the indolyl radical cation on Trp-191 (*9*). There is a distance of 16.0 Å between the closest heme macrocycle atom of yCc and the closest Trp-191 indole ring atom in CcP. A semiclassical relationship for long-range electron transfer developed by Marcus is given in eq 3 (*36*, *37*):

$$k_{et} = \frac{4\pi^2 H_{AB}{}^2}{h(4\pi\lambda RT)^{1/2}} \exp[-(\Delta G^{\circ\prime} + \lambda)^2/4\lambda RT] \quad (3)$$

where H_{AB} is the electronic coupling and λ is the nuclear reorganization energy. Dutton and co-workers have found that in a wide range of biological systems k_{et} decreases exponentially with the distance between the redox centers according to eq 4 (*38*):

$$k_{et} = k_o \exp[-\beta(r - r_o)] \exp[-(\Delta G^{\circ\prime} + \lambda)^2/4\lambda RT)] \quad (4)$$

where r is the distance between the closest macrocycle atoms in the two redox centers, the van der Waals contact distance $r_o = 3.6$ Å, β is taken to be 1.4 $Å^{-1}$, and the nuclear frequency k_o is 10^{13} s^{-1} (*38*). When the driving force $-\Delta G^{\circ\prime}$ equals the reorganization energy λ, k_{et} reaches its maximum, activation-less value, k_{max}. This appears to be the case for electron transfer from heme *c* to the Trp-191 indolyl radical cation, since the rate constant is independent of temperature. With this assumption, the rate constant for electron transfer in the crystalline yCc−CcP complex (k_{et}) is calculated to be 3×10^5 s^{-1} using eq 4 (*22*). Application of the dominant pathway model developed by Beratan and co-workers (*39*) gives a k_{et} value of 2×10^5 s^{-1} for the crystalline complex (*22*). The best pathway between heme *c* and the Trp-191 indolyl radical cation consists of 11 covalent bonds and a van der Waals contact of 4.1 Å between the heme CBC methyl group and the Ala-193 methyl group. Both theoretical estimates for k_{et} are somewhat smaller than the experimental value for k_{eta} of 2×10^6 s^{-1}. The large value of k_{eta} is another indication that configurational gating is not involved in this system. The 1:1 high-affinity complex of yCc and CcP is unusually stable, with a dissociation constant of $<10^{-8}$ M at low ionic strengths (*40*). It appears that this physiological complex is optimized for efficient electron transfer at low ionic strengths, without the need for configurational gating. The configuration does not change as the ionic strength is increased to the physiological range of about 150 mM, since the value of k_{eta} is nearly constant over this range (*22*).

Electron Transfer within the Horse Ru-27-Cc−CcP Complex. The mechanism for photoinduced electron transfer in the horse Ru-27-Cc−CcP complex shown in Scheme 3 makes use of the unique redox properties of the ruthenium trisbipyridyl complex in two different steps. First, the excited-state Ru^{II*} is a strong reducing agent ($E^\circ = -0.84$ V for the Ru^{II*}/Ru^{III} couple) which rapidly transfers an electron to heme *c* Fe^{III} to form Fe^{II} and Ru^{III}. Second, Ru(III) is a strong oxidizing agent ($E^\circ = 1.3$ V for the Ru^{III}/Ru^{II} couple) which oxidizes the indole group of Trp-191 to an indolyl radical cation to form the state CMPII(Fe^{III},$Trp^{\bullet+}$). The final electron transfer reaction, from heme *c* Fe^{II} to the Trp-191 indolyl radical cation in Scheme 3, has the same rate constant as the intracomplex electron transfer from Ru-27-Cc to the radical cation in CMPI(Fe^{IV}=0,$Trp^{\bullet+}$) (*31*). Studies in which a series of CcP surface mutations were used have shown that Ru-27-Cc binds to CcP at the same interaction domain identified in the crystal structure of the hCc−CcP complex (*31*).

The rate constant k_4 for electron transfer from heme *c* Fe^{II} to the Trp-191 indolyl radical cation in the Ru-27-Cc−CcP complex decreases with increasing viscosity, indicating that this step in Scheme 3 is gated. In contrast, the rate constant k_3 for electron transfer from the Trp-191 indole group to Ru^{III} is independent of both viscosity and temperature over a wide range, indicating that this step in Scheme 3 is not

Scheme 4

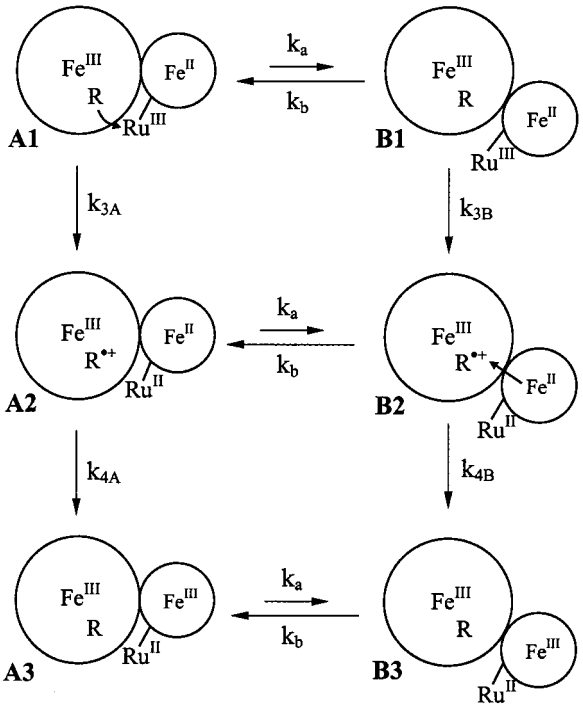

gated. It is unusual to have both gated and nongated electron transfer reactions within a single protein complex. In the simplest model consistent with these results, it is assumed that the configuration of the Ru-27-Cc−CcP complex undergoes rapid interconversion between a major state A and a minor state B (Scheme 4). For simplicity, it is assumed that state A has the configuration of the horse Cc−CcP crystalline complex, while the minor state B has the configuration of the yeast Cc−CcP crystalline complex (Figure 7). In the hCc−CcP complex, state A, the Cc molecule is rotated and translated relative to its orientation in the yCc−CcP complex so that a 3.0 Å gap is opened between the CBC heme methyl group of Cc and Ala-193, and the distance *r* between the closest macrocycle atom in heme *c* and the closest atom in the Trp-191 indole group is increased to 20.5 Å (Figure 7A). This decreases the rate constant calculated using eq 4 for electron transfer from heme *c* to the Trp-191 indolyl radical cation to $k_{4A} = k_{et} = 5 \times 10^2$ s^{-1}. Moreover, in state A a ruthenium label attached to N_ϵ of Lys-27 can be placed in van der Waals contact with the methyl side chain of Ala-193 without perturbing the interface of the crystalline hCc−CcP complex (Figure 7A). The distance from the closest atom of the ruthenium label to Ala-193 CB is about 4 Å, which would provide an efficient pathway for electron transfer between Ru^{III} and the Trp-191 indole group. Calculations using eq 4 indicate that this pathway is consistent with the large rate constant for this reaction ($k_3 = 7 \times 10^6$ s^{-1}). Thus, state A is characterized by a large rate constant k_{3A} for electron transfer between Ru^{III} and the Trp-191 indole, but a small rate constant k_{4A} for electron transfer from heme *c* to the Trp-191 indolyl radical cation. In contrast, state B is assumed to have the configuration of the yCc−CcP complex, which has a very efficient pathway for electron transfer from heme *c* to the Trp-191 radical cation, with a k_{4B} of 2×10^6 s^{-1}. To attain this configuration, the ruthenium label on Lys-27 must move further away from Ala-194, resulting in a small value for k_{3B} (Figure 7B).

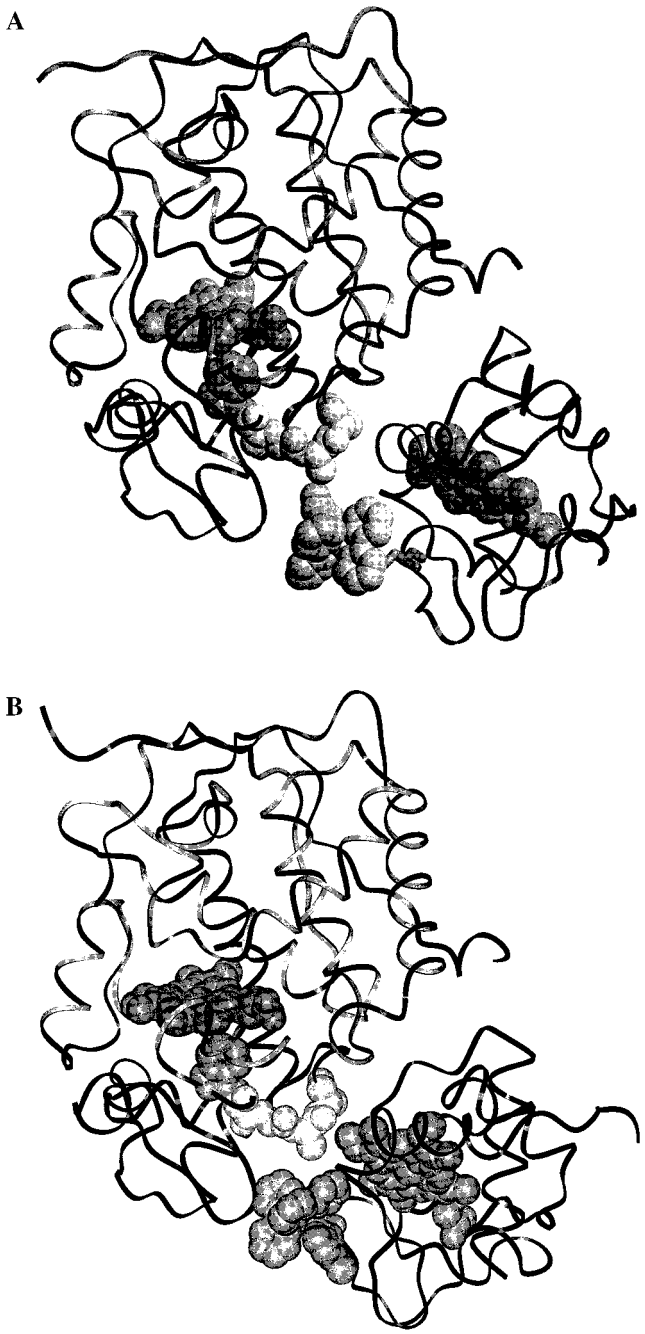

FIGURE 7: Configurational gating model for the Ru-27-Cc−CcP complex. (A) The crystal structure of the horse Cc−CcP complex with the heme groups and residues 191−194 represented by CPK models. A model of ruthenium trisbipyridyl was attached to lysine 27 and its conformation adjusted manually to place it in van der Waals contact with the methyl side chain of Ala-193 without causing any steric problems at the complex interface. (B) The crystal structure of the yeast Cc−CcP complex shown in the same orientation as shown in panel A. The ruthenium group had to be moved further away from Ala-193 to avoid contact with the complex interface.

Simulations of Scheme 4 were carried out using numerical integration methods (*31*), assuming that $k_{4B} = 2 \times 10^6$ s^{-1} and $k_{4A} = 5 \times 10^2$ s^{-1}. A good fit to the experimental value for k_4 of 6.1×10^4 s^{-1} in the absence of glycerol was obtained with a k_a of 9×10^4 s^{-1}, a k_b of 9×10^5 s^{-1}, and a K ($=k_b/k_a$) of 10. Under these conditions, 91% of the

complex is in state A, and the reaction takes place predominantly along the pathway A1 → A2 → B2 → B3 in Scheme 4. The electron transfer rate constant k_4 is gated by the rate constant k_a for the conversion of state A to state B. The experimental value of k_3 (7×10^6 s^{-1}) is equal to k_{3A}, and is not gated by k_a or k_b. However, if the value of K was decreased below 4, it was necessary to increase the value of k_{3A} to unrealistically high values. At the other extreme, a maximum value for K of 33 could be obtained in the rapid exchange limit where k_a and k_b are much larger than k_{4B}, but k_4 would no longer be gated (*2*). Realistic fits to the experimental data in the absence of glycerol were thus obtained over the following ranges: $5 < K < 15$ and 7×10^4 s^{-1} $< k_a < 10 \times 10^4$ s^{-1}.

The viscosity dependence of k_4 is consistent with Scheme 4, with the reaction gated by k_a. At 20 °C, k_4 decreases from 6.1×10^4 s^{-1} at a viscosity of 1.0 cP to 3.4×10^3 s^{-1} at 84 cP, consistent with an equivalent decrease in k_a (Figure 3). The viscosity dependence was fitted to the modified Kramer's equation (eq 1) using three parameters, $\Delta G^{\ddagger}$, σ, and k_{4A} (Figure 3). The parameter k_{4A} represents the rate of electron transfer in state A at infinite viscosity where conversion from state A to state B is prevented. It was only possible to measure an upper limit for k_{4A} of 1000 s^{-1}, which is consistent with the rate constant of 500 s^{-1} for electron transfer in state A predicted by eq 4. The value for the protein friction ($\sigma = 4.0$ cP) is comparable to the values measured for the ZnCc−plastocyanin and ZnCc−cytochrome b_5 complexes (*3*−*5*). The activation parameters ($\Delta H^{\ddagger} = 22.6 \pm 1.4$ kJ/mol and $\Delta S^{\ddagger} = -76 \pm 5$ J mol^{-1} K^{-1}) obtained from the temperature dependence of k_4 are also consistent with gating by protein−protein reorientation (*4*−*6*). Fitting the temperature dependence of k_4 with the Marcus equation (eq 3) gives a reorganization energy λ of 1.9 eV, which is much larger than the value of 0.5−0.9 eV predicted for the elementary electron transfer step in this system (*22*). It is clear from both the temperature and viscosity dependence of k_4 that this rate constant is controlled by configurational gating rather than by the elementary electron transfer event.

The location of the binding domain on CcP for several different forms of Cc has been studied using CcP surface residue mutations (*22*, *23*, *30*, *31*, *41*). The effects of these mutations on the interaction with horse and yeast Cc are essentially the same, indicating that both forms of Cc bind to the same site on CcP (*30*). There is simply a difference in the orientation of hCc and yCc at this binding site as revealed by the Pelletier−Kraut crystal structures (*9*). The CcP surface mutations also have the same effects on the interaction with Ru-27-Cc, indicating that this derivative binds to the same site on CcP (*31*). The D34N mutation has the largest effect on the interaction with all forms of Cc, leading to a more than 10-fold increase in the dissociation constant of the complex with Ru-27-Cc (*31*). Unlike the other mutations studied, D34N increases k_4 to a value of 1.3×10^5 s^{-1} at a viscosity of 1 cP. This observation suggests that eliminating the electrostatic interaction between Asp-34 and Cc lysine groups allows Ru-27-Cc to reorient more rapidly from state A to state B, increasing the value of k_a. The E290N mutation led to a 10-fold increase in the dissociation constant for the complex with Ru-27-Cc, but k_4 was decreased to 4.0×10^4 s^{-1}, indicating a decrease in the value of k_a. The k_4 values of all the mutants decreased with increasing viscosity, consistent with the proposed gating mechanism. There is a concern that the ruthenium trisbipyridyl group might cause a change in the orientation of Ru-27-Cc at the binding site, raising the question of whether gating is a factor in the reaction of native horse Cc. Studies with a series of horse Ru-Cc derivatives labeled at lysines on the back surface of the protein indicate that the rate constant k_{eta} for electron transfer to the Trp-191 radical cation by native horse Cc is approximately 10^5 s^{-1} (*42*). This value is more than 200-fold greater than the k_{et} value of 5×10^2 s^{-1} predicted for the crystalline horse Cc−CcP complex using eq 4. Therefore, configurational gating must occur if the major configuration of the horse Cc−CcP complex in solution is the same as that in the crystal.

CONCLUSIONS

These studies provide evidence that electron transfer in the physiological complex of yCc and CcP is not controlled by configurational gating. The binding free energy for this complex is large, and examination of the crystal structure indicates that the orientation of yCc at the CcP binding site is optimized for efficient electron transfer to the Trp-191 indolyl radical cation. The observed rate constant for electron transfer from heme *c* Fe^{II} to the Trp-191 radical cation ($k_{et} = 2 \times 10^6$ s^{-1}) obtained with Ru-39-Cc is consistent with theoretical predictions based on the crystalline yCc−CcP complex. Furthermore, the rate constant is independent of both viscosity and temperature.

In contrast, it appears that electron transfer in the nonphysiological complex of hCc and CcP requires configurational gating. The binding free energy of the hCc−CcP complex is smaller than that of the yCc−CcP complex, and the orientation of the crystalline hCc−CcP complex would not allow efficient electron transfer between heme *c* and the Trp-191 radical cation. The observed rate constant obtained using horse Ru-27-Cc is much larger than theoretical predictions for the hCc−CcP complex, and depends on viscosity and temperature. A gating mechanism is proposed in which the observed rate constant is controlled by the rate of conversion of the Ru-27-Cc−CcP complex from a major state A with the configuration of the hCc−CcP crystalline complex to a minor state B with the configuration of the yCc−CcP complex.

REFERENCES

1. Hoffman, B. M., and Ratner, M. A. (1987) *J. Am. Chem. Soc. 109*, 6237−6243.
2. Davidson, V. L. (1996) *Biochemistry 35*, 14035−14039.
3. Zhou, J. S., and Kostić, N. M. (1992) *J. Am. Chem. Soc. 114*, 3562−3563.
4. Ivković-Jensen, M. M., and Kostić, N. M. (1997) *Biochemistry 36*, 8135−8144.
5. Qin, L., and Kostić, N. M. (1994) *Biochemistry 33*, 12592−12599.
6. Harris, M. R., Davis, D. J., Durham, B., and Millett, F. (1997) *Biochim. Biophys. Acta 1319*, 147−154.
7. Davidson, V. L., Jones, L. H., and Zhu, Z. (1998) *Biochemistry 37*, 7371−7277.
8. Brooks, H. B., and Davison, V. L. (1994) *Biochemistry 33*, 5696−5701.
9. Pelletier, H., and Kraut, J. (1992) *Science 258*, 1748−1755.
10. Millett, F., Miller, M. A., Geren, L., and Durham, B. (1995) *J. Bioenerg. Biomembr. 27*, 341−351.

11. Mauro, J. M., Fishel, L. A., Hazzard, J. T., Meyer, T. E., Tollin, G., Cusanovich, M. A., and Kraut, J. (1988) *Biochemistry 27*, 6243−6256.
12. Scholes, C. P., Liu, Y., Fishel, L. A., Farnum, M. F., Mauro, J. M., and Kraut, J. (1989) *Isr. J. Chem. 29*, 85−92.
13. Erman, J. E., Vitello, L. B., Mauro, J. M., and Kraut, J. (1989) *Biochemistry 28*, 7992−7995.
14. Sivaraja, M., Goodin, D. B., Smith, M., and Hoffman, B. M. (1989) *Science 245*, 738−740.
15. Miller, M. A., Han, G. W., and Kraut, J. (1994a) *Proc. Natl. Acad. Sci. U.S.A. 91*, 11118−11122.
16. Fitzgrald, M. M., Churchill, M. J., McRee, D. E., and Goodin, D. B. (1994) *Biochemistry 33*, 3807−3818.
17. Huyett, J. E., Doan, P. E., Gurbiel, R., Houseman, A. L. P., Sivaraja, M., Goodin, D. B., and Hoffman, B. M. (1995) *J. Am. Chem. Soc. 117*, 9033−9041.
18. Geren, L. M., Hahm, S., Durham, B., and Millett, F. (1991) *Biochemistry 30*, 9450−9457.
19. Hahm, S., Durham, B., and Millett, F. (1992) *Biochemistry 31*, 3472−3477.
20. Durham, B., Pan, L. P., Long, J., and Millett, F. (1989) *Biochemistry 28*, 8659−8665.
21. Liu, R.-Q., Hahm, S., Miller, M. A., Han, G. W., Geren, L., Hibdon, S., Kraut, J., Durham, B., and Millett, F. (1994) *Biochemistry 33*, 8678−8685.
22. Wang, K., Mei, H., Geren, L., Miller, M. A., Saunders, A., Wang, X., Waldner, J. L., Pielak, G. J., Durham, B., and Millett, F. (1996) *Biochemistry 35*, 15107−15119.
23. Mei, H., Wang, K., McKee, S., Wang, X., Waldner, J. L., Pielak, G. J., Durham, B., and Millett, F. (1996) *Biochemistry 35*, 15800−15806.
24. Hahm, S., Geren, L., Durham, B., and Millett, F. (1993) *J. Am. Chem. Soc. 115*, 3372−3373.
25. Hahm, S., Miller, M. A., Geren, L., Kraut, J., Durham, B., and Millett, F. (1994) *Biochemistry 33*, 1473−1480.
26. Matthis, A. L., Vitello, L. B., and Erman, J. E. (1995) *Biochemistry 34*, 9991−9999.
27. Nuevo, M. R., Chu, H.-H., Vitello, L. B., and Erman, J. E. (1993) *J. Am. Chem. Soc. 115*, 5873−5874.
28. Summers, F. E., and Erman, J. E. (1988) *J. Biol. Chem. 263*, 14267−14275.
29. Miller, M. A. (1996) *Biochemistry 35*, 15791−15799.
30. Miller, M. A., Liu, R.-Q., Hahm, S., Geren, L., Hibdon, S., Kraut, J., Durham, B., and Millett, F. (1994) *Biochemistry 33*, 8686−8693.
31. Liu, R., Hahm, S., Miller, M., Durham, B., and Millett, F. (1995) *Biochemistry 34*, 973−983.
32. Geren, L. M., Beasley, J. R., Fine, B. R., Saunders, A., Hibdon, S., Pielak, G. J., Durham, B., and Millett, F. (1995) *J. Biol. Chem. 270*, 2466−2472.
33. Pan, L. P., Durham, B., Wolinska, J., and Millett, F. (1988) *Biochemistry 27*, 7180−7184.
34. Fishel, L. A., Villafranca, J. E., Mauro, J. M., and Kraut, J. (1987) *Biochemistry 26*, 351−360.
35. Margoliash, E., and Frohirt, N. (1959) *Biochem. J. 71*, 570−575.
36. Marcus, R. A. (1956) *J. Chem. Phys. 24*, 966−989.
37. Marcus, R. A., and Sutin, N. (1985) *Biochim. Biophys. Acta 811*, 265−322.
38. Moser, C. C., Keske, J. M., Warncke, K., Farid, R. S., and Dutton, P. L. (1992) *Nature 355*, 796−802.
39. Beratan, D. N., Betts, J. N., and Onuchic, J. N. (1992) *J. Chem. Phys. 96*, 2852−2855.
40. Kang, C. H., Ferguson-Miller, S., and Margoliash, E. (1983) *J. Biol. Chem. 252*, 919−926.
41. Miller, M. A., Geren, L., Han, G. W., Saunders, A., Beasley, J., Pielak, G. J., Durham, B., Millett, F., and Kraut, J. (1996) *Biochemistry 35*, 667−673.
42. Liu, R. Q., Geren, L., Anderson, P., Fairris, J. L., Peffer, N., McKee, A., Durham, B., and Millett, F. (1995) *Biochimie 77*, 549−561.
43. Weast, R. C., Ed. (1972) *Handbook of Chemistry and Physics*, The Chemical Rubber Co., Cleveland, OH.
44. Litovitz, T. A. (1952) *J. Chem. Phys. 20*, 1088.

BI983002T